Quantitative study on the modal parameters estimated using the PLSCF and the MITD methods and an automated modal analysis algorithm

Silas Sverre Christensen[1], Stefano Manzoni[2], Marcello Vanali[3], Alfredo Cigada[2], Anders Brandt[1]

[1]Department of Technology and Innovation, University of Southern Denmark,
Campusvej 55, 5230, Odense M, Denmark
[2]Politecnico di Milano, Department of Mechanical Engineering,
Via La Masa, 34 - 20156 Milan, Italy
[3]Università degli Studi di Parma, Department of Engineering and Architecture,
Parco Area delle Scienze, 181/A - 43124 Parma, Italy

ABSTRACT

There are many advanced algorithms used to estimate modal parameters. In this paper, the modal parameters extracted from the Poly-reference Least Squares Complex Frequency (PLSCF) algorithm and the Multi-reference Ibrahim Time Domain (MITD) algorithm, are compared. The former, is widely used in the industry and is known to produce almost crystal clear stabilization diagrams with barely any spurious pole estimates. The latter, is less common and the stabilization diagrams typically contain some spurious pole estimates. An Automated Modal Analysis (AMA) algorithm, that utilizes the statistical representation of the pole estimates combined with a number of decision rules based on the Modal Assurance Criteria (MAC), is employed, to detect probable physical poles. Simulated data from a Plexiglas plate is used in the study. Results indicate that the absolute bias error associated with the modal parameter estimates output by the PLSCF algorithm is higher than the bias error related to the modal parameter estimates output by the MITD algorithm. It was not conclusive which of the two methods that had the lowest random error. It should also be mentioned that, while the MITD algorithm could process all references and responses, the PLSCF algorithm relied strongly on a delicate selection of representative references and that not too many references were used.

Keywords: Automated Operational Modal Analysis, Automated Modal Analysis, Poly-reference Least Squares Complex Frequency, Multi-reference Ibrahim Time Domain, Damping.

INTRODUCTION

Modal parameters describe the dynamic properties of structures and can aid in the development of sophisticated methods for validating and updating models as well as monitoring structures during operation. There are many advanced algorithms that can be used to estimate modal parameters. Among the most popular are: Multi-reference Ibrahim Time Domain (MITD) [1] [2], Poly-reference Time Domain (PTD) [3], Eigensystem Realization Algorithm (ERA) [4], Stochastic Subspace Identification (SSI) [5], Poly-reference Least Squares Complex Frequency (PLSCF) [6], Frequency Domain Decomposition (FDD) [7] and Polyreference Frequency Domain (PFD) [8] [9].

In this paper we shall look at two of the methods mentioned, namely the PLSCF and MITD algorithms. The former is widely used in the industry and especially popular for its ability to produce very clear stabilization diagrams that produce almost no spurious information. The latter is less common and produces less clear stabilization diagrams. It may be convenient for a modal analyst when interpreting stabilization diagrams that they are clear, but there is no guarantee that a clear stabilization diagram yields the best modal parameter estimates. The time spend to interpret a stabilization diagram and select the most probably physical poles may also be inconsistent depending on the appointed operator. There are many methods available in the literature that automates this process, among some are: The K-Means (or Fuzzy-Means) Clustering algorithm [10] [11] and the Agglomerative Hierarchical Clustering algorithm [12] [13]. Some methods also utilizes the statistical representation of the pole estimates [14]

[15] [16]. In this paper an automated modal analysis (AMA) algorithm that extends from the statistical representation of the pole estimates is used. The method is extended by adding a number of decision rules based on the Modal Assurance Criterion (MAC).

The structure of this paper is as follows. In Section the general outline of the PLSCF and the MITD algorithms are described. Simulated data from a Plexiglas plate are presented in Section along with the Automated Modal Analysis (AMA) algorithm. The modal parameter estimates output by the two methods are presented in Section , and their dependencies are discussed in Section . A summary of the concluding remarks are found in Section .

THEORY

Any frequency response matrix can be decomposed into a sum of system poles, $\mathrm{s_r}$, containing damping ratios, ζ_r, and natural frequencies, $\mathrm{f_r}$, as well as a residue matrix, $\mathbf{A_r}$, which carry information about the mode shape vectors, $\boldsymbol{\psi}$, given as

$$\mathbf{H}(j\omega) = \sum_{r=1}^{N} \frac{\mathbf{A}_r}{j\omega - s_r} + \frac{\mathbf{A}_r^*}{j\omega - s_r^*} = \sum_{r=1}^{2N} \frac{\mathbf{A}_r}{j\omega - s_r} \tag{1}$$

Note that the rightmost term is but a renumbering where the sum goes to 2N instead of N, in this way, every second residue matrix is the complex conjugate of the previous residue. Information about the mode shape is retained in the numerator, while the denominator contains information about the system poles. The basic equation of an individual frequency response, $\mathrm{H_{pq}}$, can also be written as a fraction of polynomials

$$H_{pq}(\omega_i) = \frac{U_p(\omega_i)}{F_q(\omega_i)} = \frac{\beta_n(s_i)^n + \beta_{n-1}(s_i)^{(n-1)} + \cdots + \beta_0(s_i)^0}{\alpha_m(s_i)^m + \alpha_{m-1}(s_i)^{(m-1)} + \cdots + \alpha_0(s_i)^0} \tag{2}$$

where ω_i, is some measured frequency and $s_i = j\omega_i$, is the generalized frequency of the system while α and β denotes the polynomial coefficients. The order of the numerator is typically two less than the order of the denominator, i.e. n = m - 2. Rearranging Equation (2) and introducing the full frequency response matrix along with the polynomial coefficient matrices $\boldsymbol{\alpha}_k$ and $\boldsymbol{\beta}_k$ yields

$$\sum_{k=0}^{m} \boldsymbol{\alpha}_k (s_i)^k \mathbf{H}(\omega_i) = \sum_{l=0}^{n} \boldsymbol{\beta}_l (s_i)^k \tag{3}$$

Equation (3) is the frequency domain formulation using frequency response matrices. A similar expression can be derived for the time domain where impulse responses, correlation functions or random decrement signatures may be used. The force coefficients are zero, which gives

$$\sum_{k=0}^{m} \boldsymbol{\alpha}_k \mathbf{h}(t_{i+k}) = 0 \tag{4}$$

The polynomial coefficients for the frequency domain and the time domain are given in Equations (5) and (6)

$$\boldsymbol{\alpha}_m s^m + \boldsymbol{\alpha}_{m-1} s^{m-1} + \boldsymbol{\alpha}_{m-2} s^{m-2} + \cdots + \boldsymbol{\alpha}_0 = 0 \tag{5}$$

$$\boldsymbol{\alpha}_m z^m + \boldsymbol{\alpha}_{m-1} z^{m-1} + \boldsymbol{\alpha}_{m-2} z^{m-2} + \cdots + \boldsymbol{\alpha}_0 = 0 \tag{6}$$

The Poly-reference Least Squares Complex Frequency (LSCF) algorithm

The Poly-reference Least Squares Complex Frequency (PLSCF) algorithm was first formulated in [6]. It is a poly-referenced version of the Least Squares Complex Frequency (LSCF) algorithm [17], which is the frequency domain alternative to the Least Squares Complex Exponential (LSCE) algorithm [18]. The poly-referenced version of LSCE is commonly known as the Poly-reference Time Domain (PTD) algorithm [3]. The PolyMAX algorithm is similar to the PLSCF algorithm [19], yet the exact similarities are not know since the internals of the commercial implementation are not known. This paper will adopt the formulation given in [6] and [19].

The initial step of the PLSCF algorithm is to use a Right Matrix Fraction Description (RMFD) model, which is obtained by post mutiplying Equation (3) by $\sum_{k=0}^{m} \boldsymbol{\alpha}_k^{-1} (j\omega_i)^k$ yielding

$$\mathbf{H}(\omega_i) = \sum_{l=0}^{n} \boldsymbol{\beta}_l (j\omega_i)^k \sum_{k=0}^{m} \boldsymbol{\alpha}_k^{-1} (j\omega_i)^k \tag{7}$$

where the matrix polynomial $\boldsymbol{\alpha}_k(j\omega_i)^k$ and $\boldsymbol{\beta}_l(j\omega_i)^k$ have $\mathrm{N_o}\times\mathrm{N_i}$ and $\mathrm{N_o}\times\mathrm{N_o}$ coefficients, respectively. Here $\mathrm{N_o}$ denote the number of responses while $\mathrm{N_i}$ denote the number of references. The number of references are typically lower than the number of responses. For the RMFD model the number of eigenvalues equal $\mathrm{mN_i}$.

The basic concept of the PLSCF algorithm is to solve a least squares problem by minimising a cost function from an error function that is derived from Equation (7). These steps are not included in this paper, but are found in [6] and [19], where it is shown that the error function is only linear for $\mathrm{N_i}=1$ and otherwise non-linear. This is undesirable as $\mathrm{N_i}$ typically is higher than one. By some algebraic manipulation, also left out in this paper, the non-linear error function can be approximated by a linear error function. A cost function can then be formulated based on the linearised error function. The cost function is minimized by setting its derivatives with respect to the unknown polynomial coefficients, θ, equal to zero. This gives us the following reduced normal equations

$$2Re\begin{bmatrix}\mathbf{X}_1^H\mathbf{X}_1 & \mathbf{0} & \cdots & \mathbf{X}_1^H\mathbf{Y}_1\\ \mathbf{0} & \mathbf{X}_2^H\mathbf{X}_2 & & \mathbf{X}_2^H\mathbf{Y}_2\\ \vdots & & \ddots & \vdots\\ \mathbf{Y}_1^H\mathbf{X}_1 & \mathbf{Y}_2^H\mathbf{X}_2 & \cdots & \sum_{k=1}^{N_iN_o}\mathbf{Y}_k^H\mathbf{Y}_k\end{bmatrix}\begin{Bmatrix}\boldsymbol{\beta}_1\\ \boldsymbol{\beta}_2\\ \vdots\\ \boldsymbol{\beta}_{N_iN_o}\\ \boldsymbol{\alpha}\end{Bmatrix}=2Re(\mathbf{J}^H\mathbf{J})\boldsymbol{\theta}=\mathbf{0} \tag{8}$$

with J being the Jacobian matrix where $\mathrm{X_k}$ and $\mathrm{Y_k}$ depend on the polynomial basis function as well as the estimated frequency response matrices. A weighting function that accounts for the quality of the measured frequency responses matrices can also be included in Equation (8).

By setting the $\boldsymbol{\beta}_1...\boldsymbol{\beta}_{N_iN_o}$ polynomial coefficients equal to zero, the $\boldsymbol{\alpha}$ polynomial coefficients can be solved. Hereafter $\boldsymbol{\beta}_1...\boldsymbol{\beta}_{N_iN_o}$ may be found. In this way, the denominator of Equation (2), which contains the pole estimates are determined first. Then the $\boldsymbol{\beta}_1...\boldsymbol{\beta}_{N_iN_o}$ polynomial coefficients, i.e. the modal participation factors (or mode shape vectors) can be estimated.

A common way of solving the polynomial coefficient $\boldsymbol{\alpha}$ is by using the companion matrix formulation, given as

$$\mathbf{C}=\begin{bmatrix}-\boldsymbol{\alpha}_{m-1} & -\boldsymbol{\alpha}_{m-2} & \cdots & -\boldsymbol{\alpha}_0\\ \mathbf{I} & \mathbf{0} & \cdots & \mathbf{0}\\ \mathbf{0} & \mathbf{I} & \cdots & \mathbf{0}\\ \vdots & & & \vdots\\ \mathbf{0} & \cdots & \mathbf{I} & \mathbf{0}\end{bmatrix} \tag{9}$$

To solve Equations 5 and 6, it is normal to set $\boldsymbol{\alpha}_m=1$. It was, however, found in [20], that by utilizing a low order normalization, i.e. setting $\boldsymbol{\alpha}_0=1$ in Equation 5, very clear stabilization diagrams were obtained when using the PLSCF algorithm.

The PLSCF algorithm presented does not use Singular Value Decomposition (SVD), and it should not be needed, if an appropriate number of references is selected and the number of references are limited to only a few references [20]. It was pointed out in [21] that the PTD algorithm (time domain alternative to the PLSCF algorithm) produces bad stabilization diagrams when the number of references exceeds more than 3.

A Left Matrix Fraction Description (LMFD) model can also be used, but that would yield $\mathrm{mN_o}$ eigenvalues, and since $\mathrm{o}>>\mathrm{i}$, the use of the SVD (or any other equation condensation) is then advised.

The Multi-reference Ibrahim Time Domain (MITD) algorithm

The Multi-reference Ibrahim Time Domain (MITD) algorithm [2] is a multi-reference version of the Ibrahim Time Domain algorithm [1]. This method operates in time domain thus requiring impulse response functions, correlation functions or random decrement signatures as inputs. Correlation functions are used in the present analysis. The correlation function matrix, $\mathbf{R}(\tau)$, is defined as

$$\mathbf{R}(\tau)=\mathbb{E}\left[\mathbf{y}(t)\mathbf{y}^T(t+\tau)\right] \tag{10}$$

where τ denotes the time lag given in seconds and $\mathbf{y}(\mathrm{t})=[\mathrm{y_1(t)},\mathrm{y_2(t)},...,\mathrm{y_M(t)}]^{\mathrm{T}}$ is the response vector consisting of M measurements. This means that the diagonal elements in $\mathbf{R}(\tau)$ represent the autocorrelation functions while the off-diagonal elements represent the cross-correlation functions. For the MITD method it is common to gather all the information at different time lags in a block Hankel matrix, given by

$$\mathbf{H_{nm}}(\tau) = \begin{bmatrix} [\mathbf{R}(\tau))] & [\mathbf{R}(\tau)+\Delta t)] & \cdots & [\mathbf{R}(\tau)+(m-1)\Delta t)] \\ [\mathbf{R}(\tau)+\Delta t)] & [\mathbf{R}(\tau)+2\Delta t)] & \cdots & [\mathbf{R}(\tau)+m\Delta t)] \\ \vdots & \vdots & \ddots & \vdots \\ [\mathbf{R}(\tau)+(n-1)\Delta t)] & [\mathbf{R}(\tau)+n\Delta t)] & \cdots & [\mathbf{R}(\tau)+(n+m-2)\Delta t)] \end{bmatrix} \tag{11}$$

Equation (11) can be decomposed into a mode shape matrix $\mathbf{\Psi}$, a diagonal exponential pole matrix $e^{\mathbf{s_r}t}$ and a modal participation matrix $\mathbf{L}^T$

$$H_{mn}(\tau) = \mathbf{\Psi} e^{\mathbf{s_r}t} \mathbf{L}^T \tag{12}$$

The block Hankel matrix given in Equation (11) is also formulated for $\tau + \Delta t$, i.e. $\mathbf{H_{nm}}(\tau + \Delta t)$. Using these two expressions for the block Hankel matrix and by applying some algebraic manipulation, an eigenvalue problem can be constructed. Since this eigenvalue problem is very large, it is condensed using the SVD, a tool that has shown to be powerful in removing redundant information. The modal parameters are then extracted by solving the reduced eigenvalue problem.

METHODOLOGY

Modal parameter estimates were extracted from an experimental dataset of a rectangular Plexiglass plate using the MITD algorithm. The modal parameter estimates were subsequently used to produce a simulated dataset, from which modal parameter estimates have been extracted using the PLSCF and the MITD algorithms.

The Plexiglass plate measures 533 $\times$ 321 $\times$ 20 mm and is described by 35 degrees of freedom (DOFs) in a 7 by 5 grid. See [22] for details on the experimental study whose data were also used in this paper. The modal parameters from the experimental dataset were extracted using the MITD algorithm and an Automated Modal Analysis (AMA) algorithm. The AMA algorithm, described in [23], starts with constructing a statistical representation of the pole estimates for varying model orders. It is then complemented by a number of decision rules based on the Modal Assurance Criteria (MAC). The general outline of the AMA algorithm is as follows

1. Choose a modal parameter estimation method capable of producing poles and mode shape vectors at varying model orders
2. Estimate poles at mode shape vectors at various model orders
3. Initiate the statistical representation of the pole estimates
4. Introduce an occurrence threshold and temporarily exclude modal parameter estimates below said threshold
5. Compute the MAC for each remaining bin and remove modal parameter estimates whose MAC value is poor in comparison to the MAC values of the majority of poles in a given bin
6. Combine adjacent bins whose MAC values are similar
7. Add any adjacent modal parameters that did not pass step 4) to a bin if the MAC values are similar
8. Compute mean values and standard deviation for each remaining bin

The AMA algorithm has shown successful in detecting structural modes from datasets on several real structures, e.g. the Little Belt Suspension Bridge, the Heritage Court Tower and a Ro-Lo ship [23]. The modal parameter estimates from the experimental dataset using the AMA algorithm, were then used to simulated 300 s forced response sequences at a sampling frequency of 5000 Hz using superposition and digital filter theory [24]. Gaussian white noise processes were used as input in all 35 DOFs with a noise level corresponding to 0.01 % of the standard deviation of the forced response.

The simulated data were input into the PLSCF algorithm and the MITD algorithm to estimate modal parameters. A model order of 100 was used for both algorithm, to ensure that many modal parameters were output.

For the PLSCF algorithm three of the four corner points were used as references of the 35 responses. The correlation function estimates used to compute the spectral densities were postmultiplied by an exponential window so that the correlation function value at the end of the measurement time was reduced to 0.01 %. This is a common procedure used to reduce the bias error added from truncations in the time domain [25]. A total of 100 averages were used to compute the spectral density estimates. The damping ratio added from applying an exponential window was subtracted from the estimated damping ratios output by the PLSCF algorithm.

For the MITD algorithm an unbiased Welch estimator with a blocksize of 512 samples, was used to compute the correlation functions for all 35 measurement channels. The first 15 time lag values were removed from all correlation functions to suppress measurement noise [26]. Exactly 90 time lag values from each of the 1225 correlation functions were used as input into the MITD algorithm. At this point the correlation functions had almost fully decayed.

For the modal parameter estimates output by both algorithm, only poles originating from an under-damped system were considered, i.e. having low damping and positive frequency. Furthermore, damping ratio estimates above 10 % were discarded since the damping ratio of the plexiglass plate does not exceed 3.5 % for any of the modes of interest.

RESULTS

The modal parameters estimated using the two algorithms are presented in the following. The stabilization diagrams are seen in Figures 1 and 2.

In the present work, when using the PLSCF algorithm, it was crucial that a representative number of references were chosen and that the number of references were limited to only a few. The most clear stabilization diagram were obtained by choosing three of the four corner points as references, which was also mentioned in Section . By choosing more references, the number of spurious poles present in the stabilization diagrams would rise. It was attempted to use 35 references, which rendered the stabilization diagram completely indecipherable for the AMA algorithm to interpret. This observation is related to the fact that the number of eigenvalues estimated equals $\mathrm{mN_i}$, where m is the number of frequency lines and $\mathrm{N_i}$ denotes the number of references. By increasing the number of references more eigenvalues are estimated as a multiple of the number of frequency lines. Therefore, if too many references (e.g. SVD) are used, equation condensation should be employed, while, when only a few references are used equation condensation should not be required.

For the PLSCF algorithm nine modes were identified, which correspond to the number of modes used to simulate the data. It is quite clear that the frequency component of the pole estimates stabilize for increasing model order and that barely any spurious pole estimates are present. This is in line with previous observations, that very clear stabilization diagrams are output, when using the PLSCF algorithm, that was presented in Section . Upon zooming onto the first two and closely spaced modes in the same plot, it is seen, up to a model order of 20, that the model parameters are not stabilizing well on the frequency axis. Above a model order of 50 it appears that the estimates are strongly frequency stable. In the intermediate rage, model order ranging from 20 to 50, the frequency component of the model parameter estimates are slightly skewed to the right, yielding higher frequency estimates. It should be clarified that in Figure 1, the horizontal dashed black line corresponds to the occurrence threshold that was described in step 4), see Section . Modal parameter estimates marked as red circles does not satisfy step 4) and step 7), while modal parameter estimates denoted as blue squares does not satisfy step 5), see also Section . The remaining modal parameter estimates (and the bin they belong to), marked as green triangles, are strongly frequency stable and have high MAC similarity. Mean values and standard deviations are computed for the estimates in each of the combined bins.

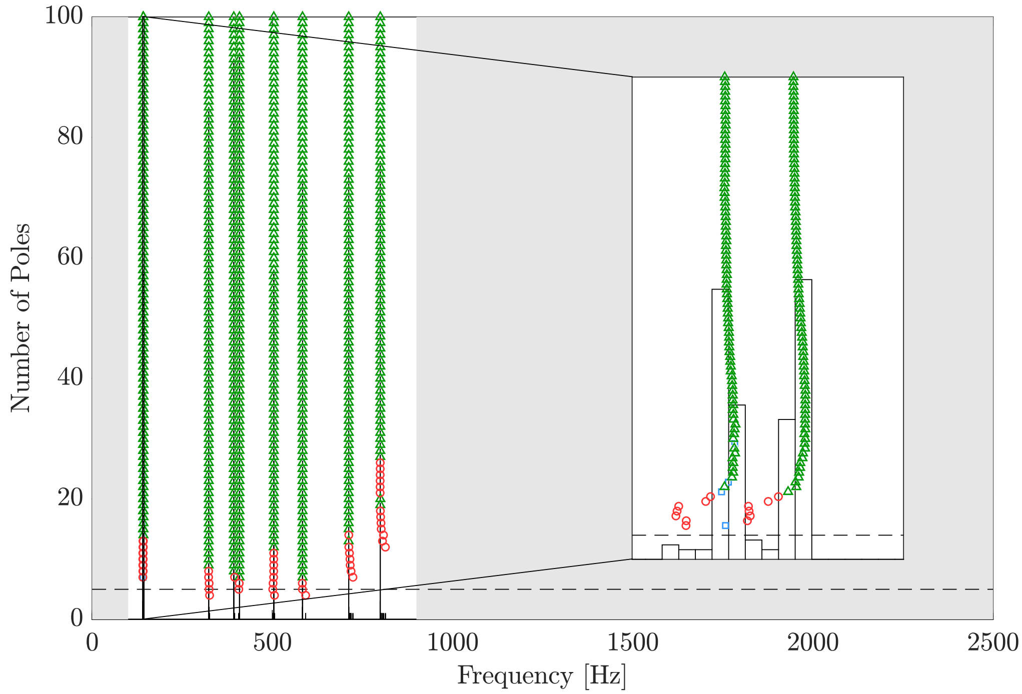

Fig. 1: Stabilization diagram overlaid by its probability mass function based on modal parameter estimates derived using the PLSCF algorithm on simulated data. ◯ circle - bins with pole estimates that are below the horizontal dashed black line and outside the white patched area; □ square - poor MAC valued pole estimates; △ triangle - stable pole estimates with similar MAC values

When looking at Figure 2 the amount of spurious information is abundant, and in direct contrast to what was seen Figure in 1, where barely any spurious information was present. It is however seen that almost no spurious information is present at the first four modes. It should be mentioned that the same nine modes that was found when using the PLSCF algorithm were also found using the MITD algorithm. When zooming onto the first two modes, it is observed that below a model order of 50 the frequency component of the pole estimates are more stable than those found when using the PLSCF algorithm. At model orders above 50 it appears that the two algorithms produced similar results.

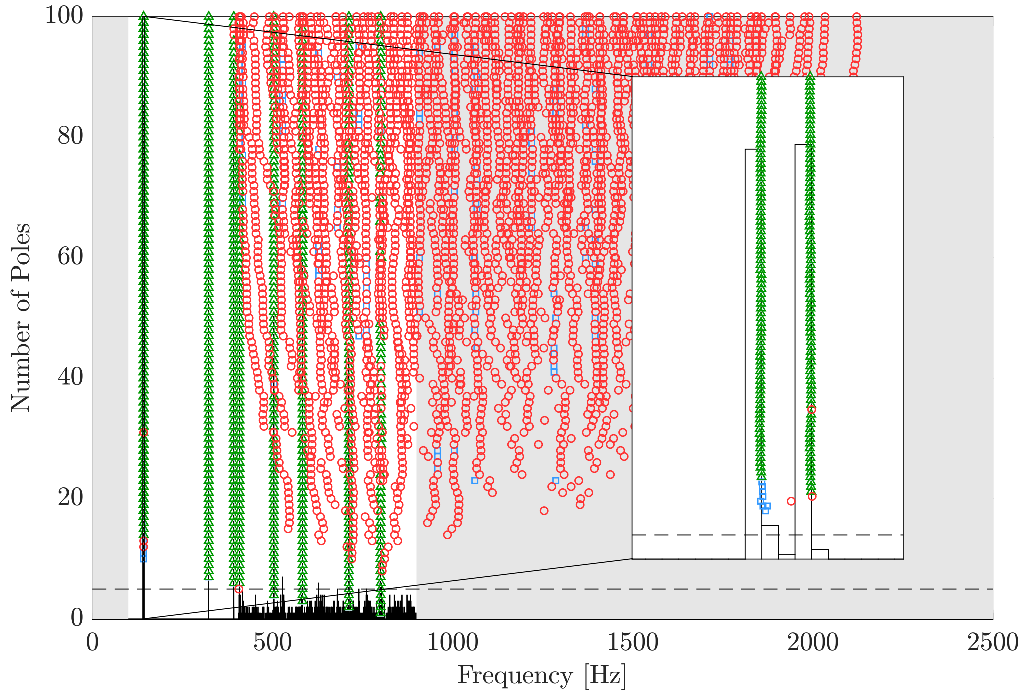

Fig. 2: Stabilization diagram overlaid by its probability mass function based on modal parameter estimates derived using the MITD method on simulated data. ◯ circle - bins with pole estimates that are below the horizontal dashed black line and outside the white patched area; □ square - poor MAC valued pole estimates; △ triangle - stable pole estimates with similar MAC values

Both methods were able to output a large number of frequency and MAC stable modal parameter estimates for the nine modes identified for different model orders. These estimates are now included in a quantitative study. In Tables 1 and 2, the number of modal parameter estimates, their mean values and standard deviations are presented. Also the mean values are compared to the true modal parameters that was used for the simulated dataset.

Upon comparing the results from the two Tables 1 and 2, it is seen that for the first three modes, the standard deviations of the modal parameter estimates output by the PLSCF algorithm are highest. Quite the opposite is seen for the last six modes, where the standard deviations of the modal parameter estimates output by the MITD algorithm are highest. When comparing the mean values of the estimates to the true values, it is evident that the relative differences, in absolute terms, are largest for the modal parameter estimates output by the PLSCF algorithm.

	Mean		Std		True		Rel. Diff. Mean		
Mode [-]	f [Hz]	ζ [%]	f [Hz]	ζ [%]	f [Hz]	ζ [%]	f [%]	ζ [%]	Count [-]
1	141.41	3.14	0.049	0.101	141.90	3.17	0.34	1.07	84
2	142.45	2.88	0.065	0.051	142.58	3.06	0.09	5.88	87
3	323.59	2.72	0.061	0.007	323.25	2.68	-0.11	-1.38	92
4	393.20	2.54	0.023	0.004	393.04	2.60	-0.04	2.38	93
5	408.95	2.50	0.025	0.016	408.73	2.53	-0.05	1.22	94
6	504.17	2.50	0.022	0.004	503.79	2.45	-0.08	-2.00	89
7	583.84	2.42	0.018	0.008	583.63	2.46	-0.04	1.75	94
8	712.05	2.39	0.056	0.029	712.01	2.42	0.00	1.40	87
9	799.69	2.18	0.038	0.044	800.09	2.22	0.05	1.58	76

Tab. 1: Mean values and standard deviations of the model parameter estimates output by the PLSCF algorithm. The relative difference on the mean value in comparison to the true value are also reported

	Mean		Std		True		Rel. Diff. Mean		
Mode [-]	f [Hz]	ζ [%]	f [Hz]	ζ [%]	f [Hz]	ζ [%]	f [%]	ζ [%]	Count [-]
1	141.89	3.14	0.018	0.010	141.90	3.17	0.00	1.07	89
2	142.67	3.09	0.018	0.016	142.58	3.06	-0.07	-0.98	87
3	323.26	2.68	0.005	0.002	323.25	2.68	0.00	0.11	94
4	392.82	2.57	0.102	0.031	393.04	2.60	0.05	1.23	93
5	408.88	2.53	0.067	0.024	408.73	2.53	-0.04	0.04	91
6	503.89	2.45	0.134	0.027	503.79	2.45	-0.02	0.04	93
7	583.57	2.50	0.291	0.139	583.63	2.46	0.01	-1.50	90
8	712.14	2.40	0.168	0.025	712.01	2.42	-0.02	0.99	96
9	800.03	2.26	0.700	0.336	800.09	2.22	0.01	-2.03	88

Tab. 2: Mean values and standard deviations of the model parameter estimates output by the MITD algorithm. The relative difference on the mean value in comparison to the true value are also reported

DISCUSSION

We have established, that the mean values of the damping ratio estimates output by the PLSCF algorithm are further from the true values, in comparison to the mean values of the damping ratio estimates output by the MITD algorithm. Although the damping ratio estimates, in absolute terms, are largest for the modal parameter estimates output by the PLSCF algorithm, it can not be concluded that the PLSCF algorithm consistently over- or underestimates the damping ratio estimates. Nor can this be said about the damping ratio estimates output by the MITD algorithm. It appears that this bias error is dependent on the mode in question. It is known that a bias error is introduced as a result of time discretization [25]. In other words, spectral leakage is the result of applying a window in the time domain prior to using the Fourier transform. Therefore a bias error is always present for any frequency domain modal parameter estimation method, including the PLSCF algorithm. However, for methods operating in the time domain, including the MITD algorithm, there is also a bias error present. This bias error is associated with the number of time lag values used in the correlation function estimates, whose optimum, is known to be different for each mode [27]. Therefore, whether the PLSCF algorithm or the MITD algorithm are used, there will always be a bias error present. The exponential window that was used in conjunction with the PLSCF algorithm, see Section , was defined so that the correlation function value at the end of the measurement time was reduced to 0.01 %. By increasing or decreasing this value by a multiple of 10, no noticeable differences were observed in the modal parameter estimates. Also for the MITD algorithm it was attempted to vary the number of time lag values used in the correlation function estimates from 70 to 130, which had minimal impact on the modal parameter estimates.

The random error for the damping ratio estimates is not definitively lower whether the PLSCF or the MITD algorithm are used. For instance high standard deviations are attributed to the damping ratio estimates for the fourth, seventh and the ninth mode when using the MITD algorithm. The standard deviation associated with the damping ratio estimates, for the first mode, is high when using the PLSCF algorithm. By taking a closer look at the frequency-damping ratio plot for this mode, seen in Figure 3, it is observed that the frequency and damping ratio estimates follow a trend. Upon further inspection it is seen that the pole estimates for the upper half (grey cross) of the stabilization diagram have lower standard deviation than those for the lower half (black plus). For the MITD algorithm the frequency and damping ratio estimates are neatly clustered, but it is also observed that the upper half of the estimates are clustered better than the lower half. Since the random error is dependent on the measurement duration, it was attempted to double the measurement time from 300 s to 600 s, which would allow twice the number of averages. This barely had any impact on the standard deviations of modal parameter estimates output by either of the two algorithms.

It was mentioned in Section and in Section , that the PLSCF algorithm is sensitive to the number of references chosen. A study [28] using the MITD algorithm showed that the modal parameter estimates were almost unaffected whether all or only a few references were used when constructing the block Hankel matrix. This is expected since the MITD algorithm employes SVD, and thus removes redundant information, making the selection of poorly located references irrelevant as long as optimal reference locations are available. It was also reported in the study that by choosing fewer references a higher variance was obtained on the modal parameter estimates. Although the PLSCF algorithm uses fewer references than the MITD algorithm, the standard deviations of the modal parameters output were not much different.

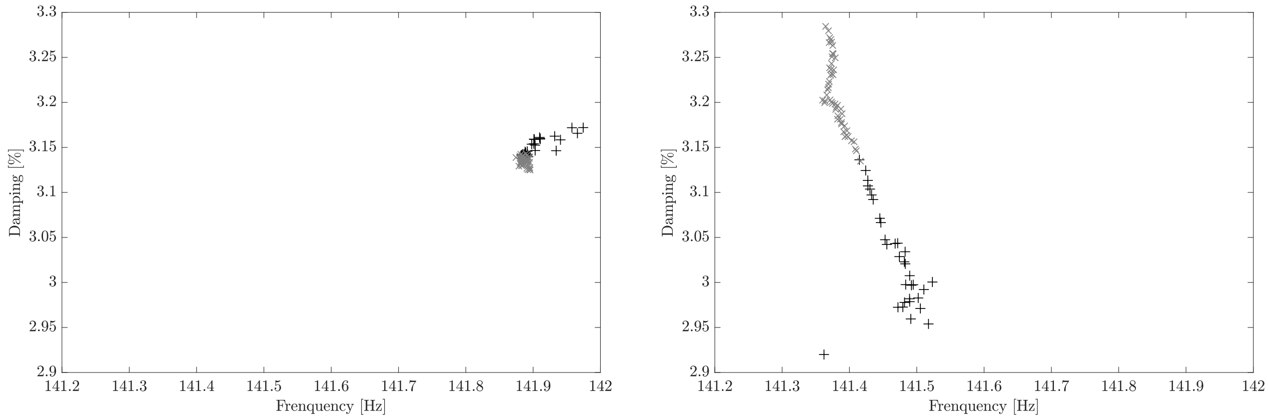

(a) **(b)**

Fig. 3: Frequency-damping ratio plot for the first mode using the modal parameters estimated from (**a**) PLSCF algorithm and (**b**) MITD algorithm. The black + (plus) denotes the lower half of the modal parameter estimates while the gray × (cross) represents the upper half of the modal parameter estimates as seen in the stabilisation diagrams, Figures 1 and 2

The frequency-damping ratio plot for the fourth mode is seen in Figure 4. As for the first mode it is seen that the upper half of the modal parameter estimates have the lowest variation when using the PLSCF algorithm. For the MITD algorithm the complete opposite is seen, compared to the behaviour observed for the first mode, that the modal parameter estimates for the lower half of the stabilization diagram have the lowest variation. For both methods, still considering the fourth mode, it is seen that a number of potential outliers are present. The outliers seem to be more profound for the modal parameter estimates output by the MITD algorithm. Potential outliers were also present for the modal parameter estimates output for the seventh and the ninth mode when using the MITD algorithm. This naturally contributes to higher standard deviations, and may also affect the mean values. By omitting the four pole estimates furthest to the right in Figure 4 **a)** and those seven pole estimates furthest to the left in Figure 4 **b)**, the variation of pole estimates appear to be similar for the two methods. However, the PLSCF algorithm still underestimates the damping ratio more than the MITD algorithm does.

Outlier detection is outside the scope of this paper, but it seems that when using a AMA algorithm, outlier detection should be employed. When an operator interprets a stabilisation diagram, that person may also assess whether one or more modal parameter estimates are deviating strongly from the majority of pole estimates. The operator would then discard those estimates in a similar manner as most outlier detecting methods would.

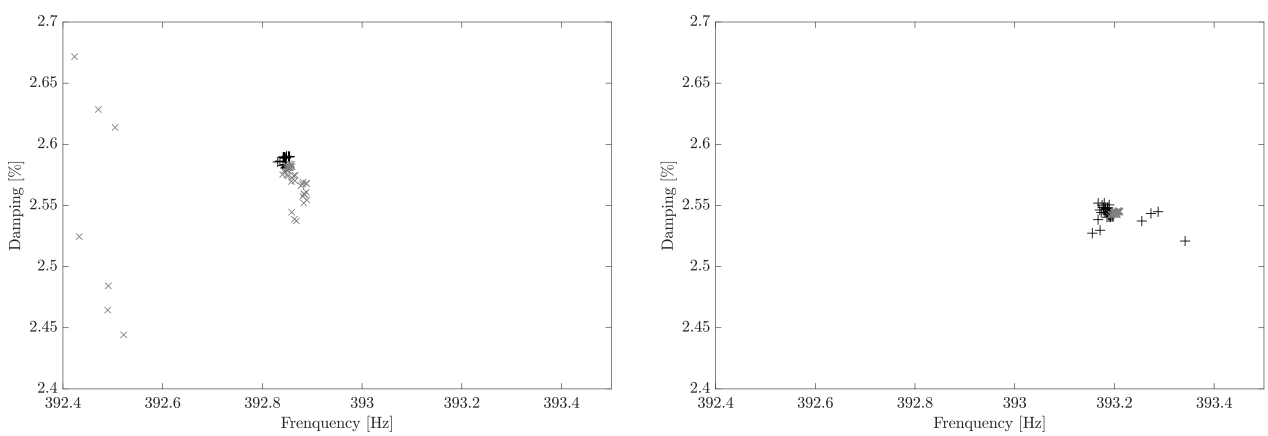

(a) **(b)**

Fig. 4: Frequency-damping ratio plot for the fourth mode using the modal parameters estimated from (**a**) PLSCF algorithm and (**b**) MITD algorithm. The black + (plus) denotes the lower half of the modal parameter estimates while the gray × (cross) represents the upper half of the modal parameter estimates as seen in the stabilization diagrams, Figures 1 and 2

CONCLUSIONS

Simulated data from a Plexiglas plate were used to estimate modal parameters using the Poly-reference Least Squares Complex Frequency (PLSCF) and the Multi-reference Ibrahim Time Domain (MITD) algorithms. An Automated Modal Analysis (AMA) algorithm based on the statistical representation of the pole estimates and complemented by a number of decision rules based on the Modal Assurance Criterion (MAC) were employed to ensure that probably physical modes were output. Upon comparing the damping ratio estimates from the two methods it was found that modal parameter estimates output by the PLSCF algorithm had higher bias, in absolute terms, in comparison to the modal parameter estimates output by the MITD algorithm. The nature of the random error associated with the damping ratio estimates was ambiguous, however, for some modes governed by outliers. It should also be mentioned that, while the MITD algorithm, can handle excess amounts of data due to the ability of the Singular Value Decomposition (SVD) to remove redundant information, the PLSCF relied on a careful selection of references and that only a few references were chosen.

ACKNOWLEDGMENTS

The work presented is supported by the INTERREG 5A Germany-Denmark program, with funding from the European Fund for Regional Development.

REFERENCES

[1] **Ibrahim, S. R.** and **Mikulcik, E. C.**, *A method for the direct identification of vibration parameters from the free response*, Shock and Vibration Bulletin 47, pp. 183–198, 1977.

[2] **Fukuzono, K.**, Investigation of multiple-reference Ibrahim Time Domain modal parameter estimation technique, Master's thesis, University of Cincinnati, 1986.

[3] **Vold, H., Kundrat, J., Rocklin, G. T.** and **Russell, R.**, *A multi-input modal estimation algorithm for mini-computers*, *Society for Automotive Engineers International Congress and Exposition*, pp. 815–821, 1982.

[4] **Juang, J.** and **Richard, P. S.**, *An Eigensystem Realization Algorithm for Modal Parameter Identification and Model Reduction*, Journal Guidance Control Dynamics, 1984.

[5] **Van Overschee, P.** and **De Moor, B.**, Subspace identification for linear systems - theory - implementation - applications, Kluwer Academic Publisher, 1996.

[6] **Guillaume, P., Verboven, P., Vanlanduit, S., Auweraer, H.** and **Peeters, B.**, *A poly-reference implementation of the least-squares complex frequency-domain estimator*, *International Modal Analysis Conference*, 2003.

[7] **Brincker, R., Zhang, L.** and **Andersen, P.**, *Modal identification from ambient responses using frequency domain decomposition*, *International Modal Analysis Conference*, pp. 625–630, 2000.

[8] **Leuridan, J. M.**, Some direct parameter model identification methods applicable for multiple input modal analysis, Ph.D. thesis, University of Cincinnati, 1984.

[9] **Zhang, L., Kanda, H., Brown, D. L.** and **Allemang, R. J.**, *A polyreference frequency method for modal parameter identification*, *American Society of Mechanical Engineers Design Engineering Technical Conference*, pp. 1237–1245, 1985.

[10] **Ubertini, F., Gentile, C.** and **Materazzi, A. L.**, *Automated modal identification in operational conditions and its application to bridges*, Journal of Engineering Structures, Vol. 46, pp. 264–278, 2012.

[11] **C., R.** and **Fabbrocino, G.**, *Development and validation of an automated operational modal analysis algorithm for vibration-based monitoring and tensile load estimation*, Mechanical Systems and Signal Processing, 2015.

[12] **Devriendt, C., Magalhães, F., Weijtjens, W., De Sitter, G., Cunha, .** and **Guillaume, P.**, *Structural health monitoring of offshore wind turbines using automated operational modal analysis*, Journal of Structural Health Monitoring, Vol. 13, No. 6, pp. 644–659, 2014.

[13] **Cardoso, R., Cury, A.** and **Barbosa, F.**, *A robust methodology for modal parameters estimation applied to SHM*, Mechanical Systems and Signal Processing, 2017.

[14] **Scionti, M., Lanslots, J., Goethals, I., Vecchio, A., Van der Auweraer, H., Peeters, B.** and **De Moor, B.**, *Tools to improve detection of structural changes from in-flight flutter data*, *International Conferenceon Recent Advances in Structural Dynamics*, 2004.

[15] **Allessandro, F.**, *Modal parameters estimation in the Z-domain*, Mechanical Systems and Signal Processing, Vol. 23, pp. 217–225, 2009.

[16] **Bakir, P. G.**, *Automation of the stabilization diagrams for subspace based system identification*, Journal of Expert Systems with Applications, Vol. 38, No. 12, pp. 14390–14397, 2011.

[17] **Auweraer, H., Guillaume, P., Verboven, P.** and **Vanlanduit, S.**, *Application of a fast-stabilizing frequency domain parameter estimation method*, ASME Journal of Dynamic Systems, Measurement, and Control, Vol. 123, No. 4, pp. 651–658, 2001.

[18] **Brown, D. L., J., A. R., Zimmerman, R.** and **Mergeay, M.**, *Parameter Estimat.ion Techniques for Modal Analysis*, SAE Transactions, Vol. 88, No. 1, pp. 828–846, 1979.

[19] **Peeters, P., Auweraer, H., Guillaume, P.** and **Leuridan, J.**, *The PolyMAX frequency-domain method: a new standard for modal parameter estimation?*, Shock and Vibration, Vol. 11, No. 3-4, pp. 395–409, 2004.

[20] **Cauberghe, B.**, Applied frequency-domain system identification techniques in the field of operational modal analysis, Ph.D. thesis, Vrije University Brussel, 2003.

[21] **Guillaume, P., Verboven, P.** and **Vanlanduit, S.**, *Frequency-domain maximum likelihood identification of modal parameters with confidence intervals*, Proceedings of the International Conference on Noise and Vibration Engineering, 1998.

[22] **Orlowitz, E.** and **Brandt, A.**, *Comparison of Experimental and Operational Modal Analysis on a Laboratory Test Plate*, Measurement, Vol. 102, pp. 121–130, 2017.

[23] **Christensen, S. S.** and **Brandt, A.**, *Automatic operational modal analysis using statistical modelling of pole locations*, Proceedings of the International Conference on Noise and Vibration Engineering, 2018.

[24] **Ahlin, K., Magnevall, M.** and **Josefsson, A.**, *Simulation of forced response in linear and nonlinear mechanical systems using digital filters*, Proceedings of the International Conference on Noise and Vibration Engineering, 2006.

[25] **Brandt, A.**, Noise and Vibration Analysis - Signal Analysis and Experimental Procedures, Wiley, 2011.

[26] **Orlowitz, E.** and **Brandt, A.**, *Influence of Noise in Correlation Function Estimates for Operational Modal Analysis*, Proceedings of International Modal Analysis Conference, 2018.

[27] **Christensen, S. S.** and **Brandt, A.**, *Parameter study of statistics of modal parameter estimates using automated operational modal analysis*, Proceedings of the 37th International Modal Analysis Conference, 2019.

[28] **Orlowitz, E.**, *Effects of sensor count on damping estimates from operational modal analysis*, Proceedings of International Modal Analysis Conference, Vol. 8, pp. 357–364, 2019.